International Journal of Nanomedicine

Dovepress
open access to scientific and medical research

Open Access Full Text Article

ORIGINAL RESEARCH

Mycosynthesis, characterization, anticancer and antibacterial activity of silver nanoparticles from endophytic fungus *Talaromyces purpureogenus*

This article was published in the following Dove Press journal:
International Journal of Nanomedicine

Xiaowen Hu[1]
Kandasamy Saravanakumar[1]
Tieyan Jin[2]
Myeong-Hyeon Wang[1]

[1]Department of Medical Biotechnology, College of Biomedical Sciences, Kangwon National University, Chuncheon 200-701, South Korea; [2]Department of Food Science and Engineering, College of Agricultural, Yanbian University, Yanji, Jilin, People's Republic of China

Background: Biogenic silver nanoparticles (AgNPs) have wider range of biomedical applications. The present work synthesized Tp-AgNPs using mycelial extract of endophytic fungus *Talaromyces purpureogenus* (MEEF), characterized, and analyzed for antibacterial, anti-proliferation and cell wounding healing activities.

Methods: The synthesized Tp-AgNPs were characterized by UV-visible spectrophotometer (UV-Vis), field emission transmission electron microscopy (FETEM) with energy-dispersive X-ray spectroscopy (EDS), Fourier transform infrared spectroscopy (FTIR), particle size analysis (PSA) and X-ray diffraction (XRD). Further, antibacterial activity was determined by Kirby–Bauer test and anti-proliferation activity was tested in human lung carcinoma A549 by water-soluble tetrazolium and flow cytometer assay. In addition, cell wounding healing activity was determined by scratch assay.

Results: UV-Vis results displayed a strong absorption peak from 390 nm to 420 nm, which indicated the successful synthesis of Tp-AgNPs. FETEM-EDS results indicated the round and triangle shaped Tp-AgNPs with the average size of 25 nm in accordance with PSA. FTIR analysis indicated the involvement of various functional molecules from MEEF in the synthesis of Tp-AgNPs. XRD result proved nature of Tp-AgNPs as a high-quality crystal. The Tp-AgNPs significantly inhibited the growth of bacterial pathogens at the minimal inhibitory concentration of 16.12 $\mu g.mL^{-1}$ for $Gram^{+}$, and 13.98 $\mu g.mL^{-1}$ for $Gram^{-}$ bacteria. Further, Tp-AgNPs (2 $\mu g.mL^{-1}$) showed a strong anti-proliferation effect in A549. Interestingly, Tp-AgNPs was not cytotoxic to normal NIH3T3 cells. In addition, the NPs exhibited a strong cell wounding healing activity.

Conclusion: This work biosynthesized AgNPs with strong antibacterial, anticancer and cell wound healing properties using endophytic fungus *T. purpureogenus*.

Keywords: mycosynthesis, silver nanoparticles, *Talaromyces purpureogenus*, antibacterial, anticancer, cell wound healing

Introduction

Nanotechnology provides a tool for synthesis of nanoparticles (NPs), which has an important role of applications in the field of biology, chemistry, physics, and medicine.[1] In biology, NPs are mainly used as carriers to form green nanoparticles with various organisms, such as the use of silver nanoparticles (AgNP) conjugated with ceftriaxone to enhance the antibacterial properties of ceftriaxone.[2] The green synthesis of AgNPs marine alga *Gelidium amansii* and bacterium *Bacillus brevis* has been reported to effectively fight against pathogens.[3,4] In physics, many

Correspondence: Myeong-Hyeon Wang
Department of Medical Biotechnology, College of Biomedical Sciences, Kangwon National University, Chuncheon 200-701, South Korea
Tel +8 233 250 6486
Fax +8 233 241 6480
Email mhwang@kangwon.ac.kr

© 2019 Hu et al. This work is published and licensed by Dove Medical Press Limited. The full terms of this license are available at https://www.dovepress.com/terms.php and incorporate the Creative Commons Attribution – Non Commercial (unported, v3.0) License (http://creativecommons.org/licenses/by-nc/3.0/). By accessing the work you hereby accept the Terms. Non-commercial uses of the work are permitted without any further permission from Dove Medical Press Limited, provided the work is properly attributed. For permission for commercial use of this work, please see paragraphs 4.2 and 5 of our Terms (https://www.dovepress.com/terms.php).

researchers use metal NPs as a special material to make nanoparticle sensors and nanoparticle switches.[5–9] The United States, the European Union, and Japan accord great importance to the research on nanomedicine.[10] The most important factor is a selection of metals for synthesizing of NPs. After more than two decades of research, the scientists have reported that the metals such as gold, silver, zinc, iron, copper, and platinum could be a potential source for the synthesis of nanomaterials.[11] Among them, the silver has been used as a traditional disinfectant and antibacterial agent since ancient times, which has attracted the interest of more workers.[12] AgNPs are also stable in physicochemical properties, including catalytic, antibacterial activity, and cytotoxicity to cancer cells.[13]

The "battle" between humans and pathogens has been going on for centuries, and a large number of human deaths have occurred due to pathogenic bacteria. Although after the discovery of the first antibiotic "penicillin", a phased victory has been achieved to combat diseases. However, with the massive abuse of antibiotics, the pathogens have evolved and developed resistance genes thereby resulting in resistance toward available antibiotics. Therefore, research is imminent to search for alternatives antibiotics.[14,15] To achieve this goal, researchers are in focus of Ag^+ that has a strong antibacterial ability through increased contact with pathogenic bacteria.[16]

Cancer has become the second leading cause of death in the world, and about 9.55 million people died of cancer so far in 2018. Among 7.6 billion people in the world, about 18 million people have cancer incidence, of which, lung cancer patients account for 11.6% as ranking first.[17] The human lung cancer cells A459 belong to human lung alveolar basal epithelial cells are currently used as a model for lung cancer and anti-lung cancer drug research.[18] The treatment of cancer cells through surgery, radiotherapy, and traditional chemotherapy are cytotoxic to normal cells and these methods are expensive, and ineffective.[19–21] In order to reduce the cytotoxicity and improve the efficiency of the chemotherapy, the synthesis of unique nanocomposites combined with anti-cancer drugs is attempted.[22] The anticancer activity of AgNPs is proved in many experiments.[23–26] However, chemically synthesized AgNPs are cytotoxic to normal human cells. Therefore, in recent years, biosynthesized AgNPs is in much focus of the researchers.

Endophytic fungi are beneficial endosymbiont not causing any disease in plants. The endophytic fungi are a good source of antibacterial and anti-cancer drugs, as evident by the first discovery of "Pseudomycin".[27] In recent years, the endophytic fungi based biosynthesis NPs are favored due to their economical, environmental friendly and stable characteristics. Compared with plants and other microorganisms, endophytic fungi are good machines for the synthesis of any type of metallic NPs because of amenability to culture conditions, extracellular enzyme secretion, rapid growth, easy production of biomass and simple operation of the endophytic fungi.[28] In the present study, we used an endophytic fungus *T. purpureogenus* isolated from leaves of *Pinus densiflora* for the synthesis of AgNPs, which were further characterized and evaluated for cell viability, antibacterial, and wound healing activities.

Materials and methods

Microorganisms and chemicals

The endophytic fungal strain *T. purpureogenus* (GenBank accession number: MK108915) was used for the synthesis of NPs. This fungal strain was previously isolated from the leaves of *Pinus densiflora* S. et Z. collected from the mountain of Kangwon National University, Chuncheon. Bacterial pathogens such as *Staphylococcus aureus* (ATCC13150), *Bacillus cereus* (KNIH28), *Salmonella enterica* (ATCC14028), *Pseudomonas aeruginosa* (ATCC27853), and *Escherichia coli* (ATCC27853) were used for the antibacterial assay. The chemicals including tartaric acid, silver nitrate ($AgNO_3$, 99.8%, Sigma, St Louis, MO, USA), water-soluble tetrazolium (WST)-1 assay kit (EZ-Cytox; Daeil Lab Service, Republic of Korea), the PBS, Roswell Park Memorial Institute medium (RPMI-1640), DMEM, FBS and Penicillin-Streptomycin (P/S) from Gibco (Waltham, MA, USA), and all chemicals were obtained from local chemical vendor, Seoul, Republic of Korea.

The human lung carcinoma, A549 cell line (KCLB-10,185) and the Swiss albino mouse embryo tissue, NIH3T3 cell line was obtained from the Korean Cell Line Bank (KCLB, Seoul, Republic of Korea). The A549 cell line cultured in RPMI-1640 and the NIH3T3 cell line cultured in DMEM, both kinds of medium containing 10% FBS and 1% PS at 37°C in a 5% CO_2 humidified incubator for 24 hrs to achieve 80–90% confluent followed by preservation in Cell Freezing Media (DMSO, BCS) in liquid nitrogen in a cryogenic vial for the experimental use.

Preparation of endophytic fungal extracts

The MEEF (mycelial extract of endophytic fungi) was prepared following standard methods.[29–31] In brief, 2 mL of fungal spore suspension (8 × 10^6spores/mL) was inoculated in 200 mL PDB in 500 mL Erlenmeyer flasks incubated at 27±2°C for 72 hrs with continuous shaking at 180 rpm. After incubation periods, the residual components of the medium in the mycelia were separated by filtration followed by washing with distilled water three times. Finally, the harvested wet fungal biomass (20–30 g) was transferred into 100 mL distilled water in 250 mL Erlenmeyer flasks and incubated at 27±2°C for 24 hrs with 180 rpm shaking for the extraction. At the end shaking process, cell-free filtrate (MEEF) was filtered using Whatman No.1 filter paper and used in further experiments.

Biosynthesis of Tp-AgNPs

The AgNPs were synthesized according to the method[32] with modifications. In brief, the synthesis of the Tp-AgNPs was initiated by adding 30 mM $AgNO_3$ in 100 mL of MEEF and the reaction mixture was incubated in shaking incubator at 27°C for 96 hrs with 180 rpm in dark. The aliquots of samples were withdrawn at different time intervals and observed for color change from white to dark brown.

Characterization of biosynthesized silver nanoparticles

The successful synthesis of Tp-AgNPs was determined by measuring the absorbance of the solution at different time intervals (1, 4, 12, 24, 48, and 96 hrs) at 300–700 nm (1 nm interval) using UV–Vis spectrophotometer (Libra S80; Biochrom Ltd, UK). After the 96 hrs reaction, the mixture was centrifuged at 12,000 rpm at room temperature for 15 mins, the supernatant was discarded, and washed by distilled water. Then, Tp-AgNPs were lyophilized and this lyophilized powder was used for further characterization using Fourier transform infrared spectroscopy (FTIR) (Frontier; PerkinElmer, Waltham, MA, USA) to detect the molecular structure and chemical bonds. The Tp-AgNPs powder was suspended in ethanol to determine the size and shape using field emission transmission electron microscopy (FETEM)–energy-dispersive X-ray spectroscopy (EDS) (JEM-2100F; Jeol, Tokyo, Japan). The size of Tp-AgNPs was determined by particle size analyzer (PSA) (model Mastersizer 3000; Malvern Instruments, Malvern, UK). Finally, X-ray diffraction (XRD) (X'Pert PRO MPD; PANalytical, Almelo, the Netherlands) was used to analyze the morphology and crystalline nature of Tp-AgNPs in a wide range of Bragg angles 2^{θ} at scanning rate 30°–80° at 0.041°/mins with a time constant of 2 s. The dielectric contents were calculated and used to study the optical properties of Tp-AgNPs as described elsewhere[33,34]

Cell viability

The cell viability was determined by WST kit assay.[35] The A459 cells were cultured in RPMI medium incorporated with 1% P/S antibiotics, 10% FBS in 5% CO_2 incubator at 37°C. After reaching the 80–90% confluence, the healthy cells were washed with PBS and then collected using Trypsin-EDTA. The 100 µL of healthy A549 cells (1 x 10^4 cells.mL^{-1}) were seeded in 96-well plate and incubated in a CO_2 incubator for 24 hrs at 37°C in 5% CO_2 incubator. After incubation, the cells were checked under the microscope to confirm the proliferation of the cells at the level of 80–90% confluence, then 10 µL different concentrations of Tp-AgNPs (0–1000 µg.mL^{-1}) were added to wells at triplicate and the cells were allowed to react with Tp-AgNPs in CO_2 incubator for 24 hrs. Then, the cytotoxicity of the Tp-AgNPs was measured by adding the 10 µL of EZ-Cytox to each well and incubated in a CO_2 incubator for 1 hrs. Finally, the samples were gently shaken for 1 min and measured the absorbance at 450 nm using a plate reader (Libra S80; Biochrom Ltd.) for calculating cell viability (%).

For the flow cytometer analysis, the IC_{50} concentration of the Tp-AgNPs was treated to A549 cells in 5% CO_2 incubator at 37°C for 48 hrs. Then, using Trypsin-EDTA the treated and untreated cells were harvested and washed by PBS to remove the Trypsin-EDTA by centrifugation. The washed cells were collected by centrifuge and dissolved in 100 µL of 1X annexin-binding buffer. For the flow cytometer reading, 5 µL of FITC annexin Vand 1 µL of PI (100 µL/mL) were added to 100 µL of A549 cell suspension. This mixture was incubated at room temperature for 15 mins. Finally, 400 µL of 1X annexin-binding buffer was added and gently mixed. The stained cells were analyzed by flow cytometry, measuring the fluorescence emission at 530 nm (eg, FL1) and >575 nm (eg, FL3).

Antibacterial

The disc diffusion method was used to determine the antibacterial activity of Tp-AgNPs according to the method described elsewhere.[36] In brief, all the bacterial strains (*S. aureus, B.cereus, S.enterica, P.aeruginosa*, and *E.coli*) were cultured in 10 mL of MHB in 50 mL

Erlenmeyer flask for overnight at 37°C. Then, 50 μL of grown bacterial cell suspensions was spreading on MHA plates. Further, the 5 mm of sterile discs saturated with either antibiotics (positive control group) and/or different concentrations of Tp-AgNPs were placed on each plate and incubated at 37°C for 24 hrs. The antibacterial activity of Tp-AgNPs was measured as clear zone inhibition (mm) using a vernier caliper.

Cell wound healing

The NIH3T3 cells (1×10^5 mL^{-1}) were cultured in 2 mL/well of DMEM supplement with 10% FBS and 1% P/S in 6-well plate, incubated in 5% CO_2 incubator at 37°C for 24 hrs. Meanwhile, different concentrations of Tp-AgNPs solution was prepared using DMEM. After incubation, the cell confluence was checked under microscope and the cells were scratched using the pipette tips, then washed with PBS. The control was replaced with normal DMEM for control, while the test group was replaced with different concentrations of Tp-AgNPs incorporated DMEM. The wound healing area was calculated at different time intervals (0–48 hrs) using a microscope and ImageJ software.

Result and discussion

Characterization of biosynthesized silver nanoparticles

In the process of biosynthesis of Tp-AgNPs, the original white reaction mixture (MEEF and $AgNO_3$) was gradually turned into brown, and the color became deeper (Figure 1A). The Tp-AgNPs was irradiated with light,

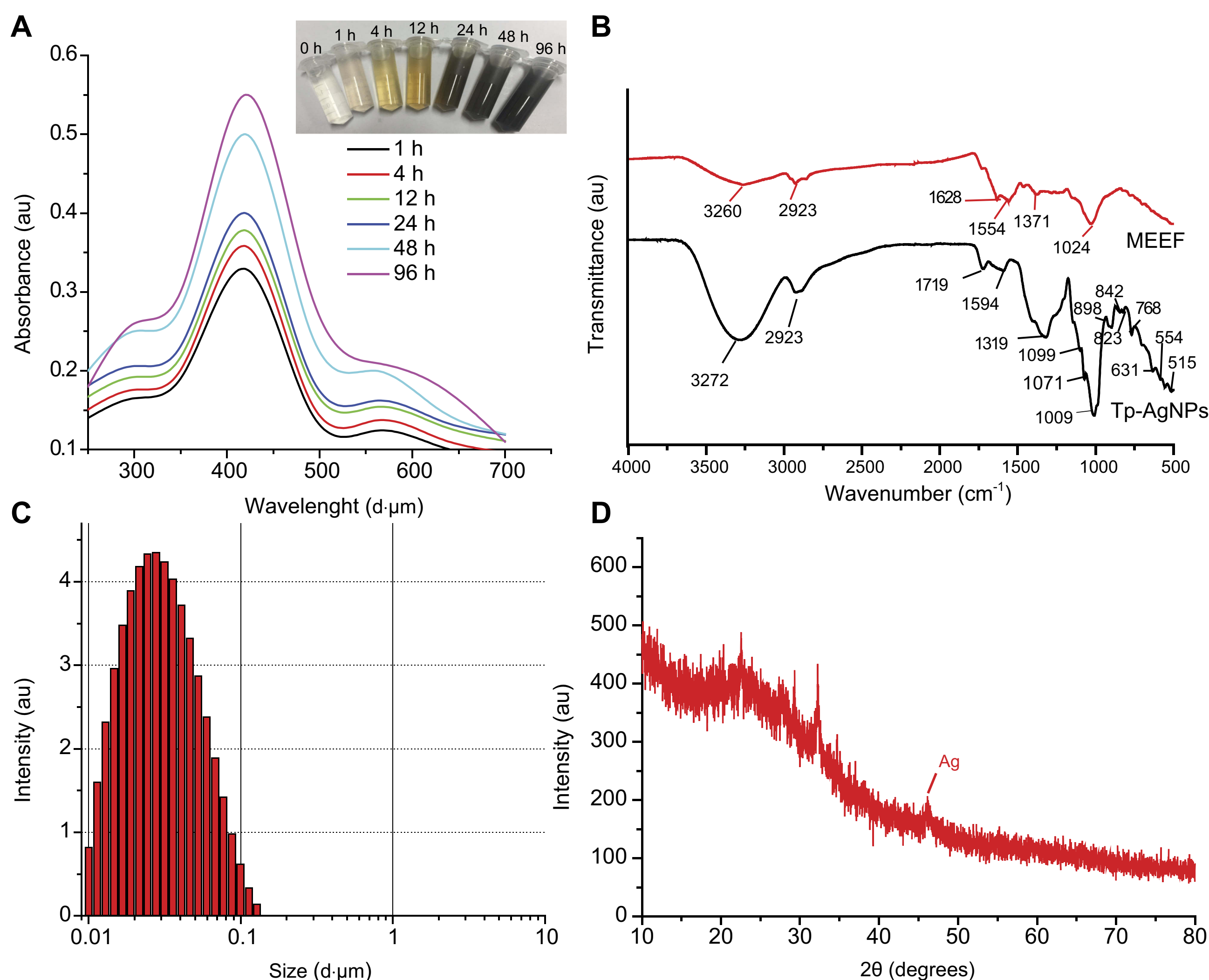

Figure 1 . Synthesis of the Tp-AgNPs using the endophytic fungi extracts and their characterization by UV-visible spectrophotometer (**A**), FTIR analysis (**B**), Particle size analysis (**C**), XRD pattern analysis (**D**).

Abbreviations: FTIR, Fourier transform infrared spectroscopy; XRD, X-ray diffraction; Tp-AgNPs, *Talaromyces purpureogenus* silver nanoparticles.

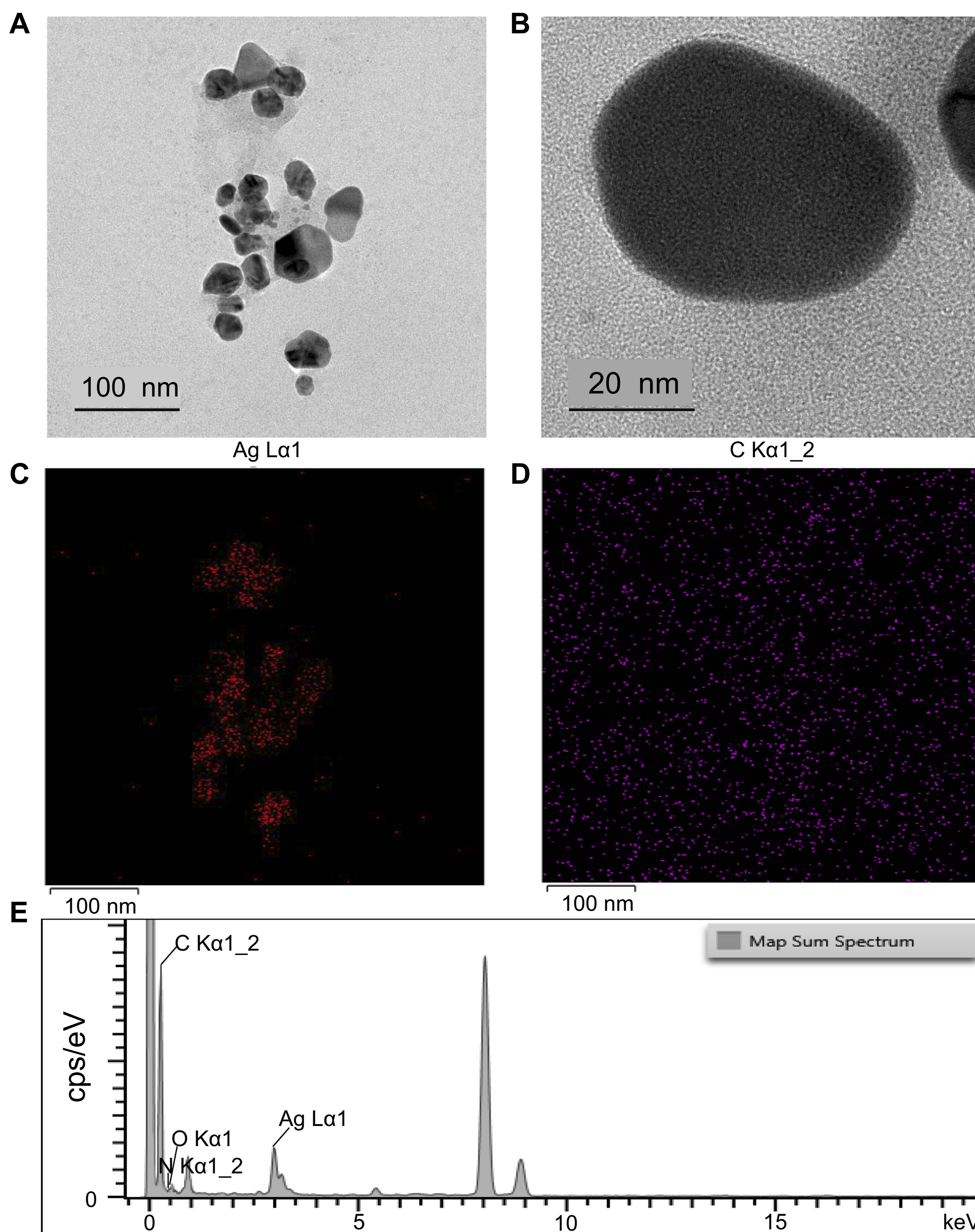

Figure 2 FETEM image of Tp-AgNPs at <100 nm (**A**) and 20 nm (**B**). EDS-based mapping of the Ag (**C**) and carbon in Tp-AgNPs (**D**). EDS chromatograph of Tp-AgNPs (**E**).
Abbreviations: FETEM, field emission transmission electron microscopy; Tp-AgNPs, *Talaromyces purpureogenus* silver nanoparticles; EDS, energy-dispersive X-ray spectroscopy; Ag, silver.

for an electronic dipole oscillation phenomenon to occur.[37–39] The strong absorption peak in the wavelength range from 390 to 420 nm with a distinct peak at around 418 nm (Figure 1A) from UV-Vis analysis indicated the successful synthesis of Tp-AgNPs in accordance with previous reports.[40]

FTIR analysis provides information about the functional groups, involved in the synthesis and/or stabilizing of Tp-AgNPs. FTIR spectrum of Tp-AgNPs (Figure 1B) showed the peak at 3260 cm^{-1} (O–H and N–H), 2923 cm^{-1} (C in C–H), 1628 cm^{-1} and 1554 cm^{-1} corresponding to the stretching vibration of the C=C, 1371 cm^{-1}

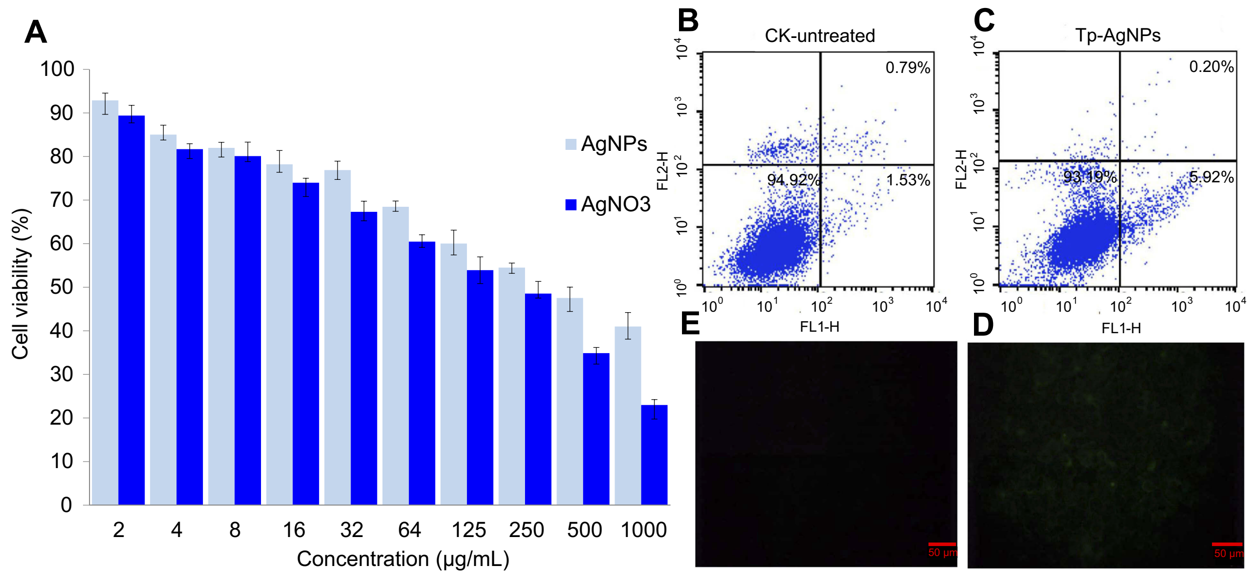

Figure 3 Cytotoxicity of Tp-AgNPs and $AgNO_3$ in A549 cells (**A**). Flow cytometry-based analysis of cell death in A549 cells untreated (**B**) and treated with Tp-AgNPs (**C**) and analysis of the ROS generation in A549 cells untreated (**E**) and treated with Tp-AgNPs (**D**).
Abbreviations: CK, control group; Tp-AgNPs, *Talaromyces purpureogenus* silver nanoparticles; AgNO3, silver nitrate; ROS, reactive oxygen species.

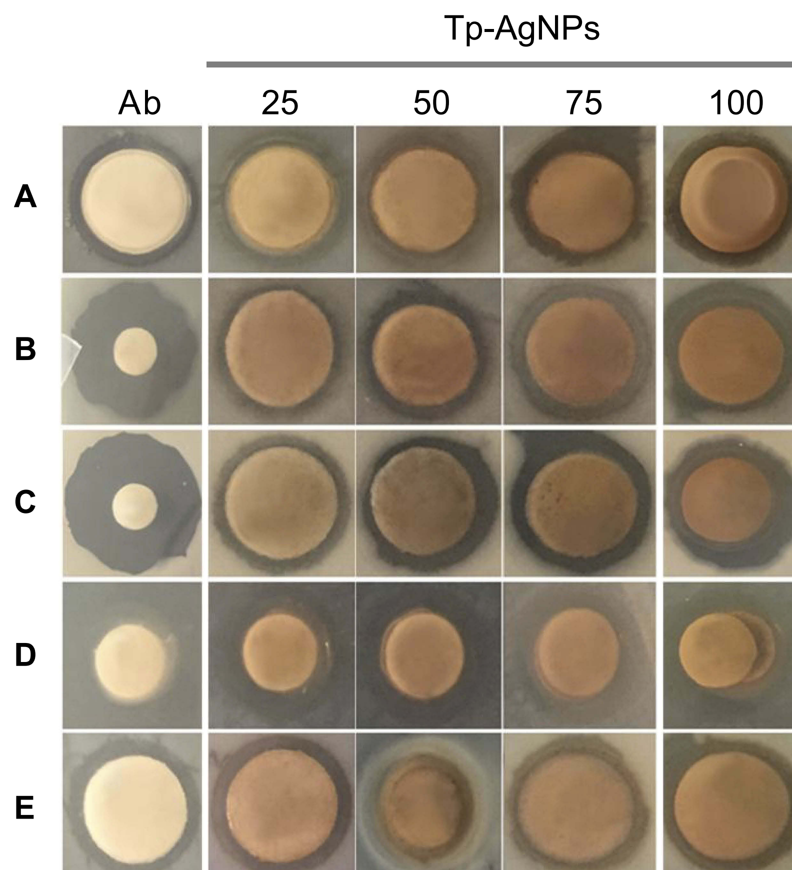

Figure 4 Antibactrial activity of Tp-AgNPs: *Staphylococcus aureus* (**A**), *Bcillus cereus* (**B**), *Salmonella entrica* (**C**), *Pseudomonas aeruginosa* (**D**), and *Escherichia coli* (**E**). Ab – vancomycin; different concentrations of Tp-AgNPs solution: 25–100 μg mL^{-1}.
Abbreviations: Tp-AgNPs, *Talaromyces purpureogenus* silver nanoparticles; Ab, vancomycin.

Table 1 Antibacterial activity of silver nanoparticles (AgNPs) synthesized by endophytic fungi

No.	Name of host plant	Name of endophytic fungi	AgNPs size (nm)	Application	Reference
1	*Solanum nigrum*	*Setosphaeria* sp.	20–50	Antibacterial	49
2	*Solanum lycopersicum* L.	*Aspergillus terreus*	45.2	Antifungal	50
3	*Salacia chinensis*	*Phomopsis liquidambaris*	18.7	Antimicrobial and larvicidal activity	51
4	*Taxus baccata* L.	*Nemania* sp.	33.52	Antibacterial	52
5	*Chetomorpha antennina*	*Penicillium polonicum* ARA 10	10–15	Antibacterial	53
6	*Withania Somnifera*	*Fusarium semitectum*	–	Antibacterial	54
7	*Simarouba glauca*	*Aspergillus niger*	41.9	Antibacterial Antioxidant Antimitotic	55
8	*Calotropis procera*	*Aspergillus terreus*	16.45	Antibacterial	56
9	*Chetomorpha antennina*	*Penicillium polonicum*	10–15	Antibacterial	57
10	*Arctostaphylos uva-ursi,* *Anabasis articulate,* *Mentha* *Cornulaca*	*Alternaria arborescens* *Alternaria alternata* *Alternaria brassicae* *Nigrospora oryzae* *Penicillium crustosum*	5–20	Antimicrobial	58
11	*Tectona grandis*	*Chaetomium globosum*	16	Antibacterial	59
12	orchids, *Dendrobium nobile,* *Dendrobium hibiki,* *Oncidium altissimum*	KDH5 VDN3B	15–25	Antibacterial	60
13	*Raphanus sativus*	*Alternaria* sp	10–30	Antibacterial	61
14	*Glycosmis mauritiana*	*Penicillium*	65	Antioxidant Antibacterial	62
15	*Psidium guajava Linn.*	*Pestaloptiopsis pauciseta*	123–195	Unknown	63
16	*Catharanthusroeus*	*Curvularia lunata*	26	Antimicrobial	64
17	*Centella asiatica*	*Aspergillus niger*	10–50	Antimicrobial	65
18	*Potentilla fulgens* L.	*Aspergillus tamari* PFL2, *Aspergillus niger* PFR6 *Penicllium ochrochloron* PFR8.	3.5 8.7 7.7	Unknown	66
19	*Curcuma longa*	*Penicillium* sp.	25–30	Antibacterial	67
20	*Rhizophora mangle* *Laguncularia racemosa*	MGE-201 L-2–2	35	Antifungal Antibacterial	68
21	*Pinus densiflora* S. et Z.	*Talaromyces purpureogenus*	<50	Antibacterial	Present study

corresponding to the expansion and contraction of C–O and C–X, 1024 cm^{-1} corresponding to the stretching vibration of C–O in the alcohol. Overall, the FTIR analysis indicated the presence of functional groups such as benzene rings, amines, and alcohols in Tp-AgNPs. The comparison of FTIR spectrum of Tp-AgNP with MEEF indicated that many of the peaks in the range of 900–500 cm^{-1} were corresponding to C-substitution stretching vibration at different positions on the benzene ring. So, biosynthesis of the NPs retained only the main functional groups of the fungus, similar to the earlier reports.[41]

The average size of the Tp-AgNPs was about 25 nm, as evident by PSA (Figure 1C). In addition, the XRD analysis indicated the 2θ values of 46° which is corresponding to Braggs's refraction value (220), and it is similar to earlier XRD report of the biosynthesized AgNPs.[42–44] Also, the present results compared with the general AgNPs, the 2θ value obtained in this experiment was similar at the peak of 46° belonging to the characteristic peak of AgNPs (Figure 1D). Most of the Tp-AgNPs were dispersed, round, triangles shaped and sized <50 nm (Figure 2A,B), as revealed by TEM-EDS. The EDS

Table 2 Zone of inhibition of produced by Tp-AgNPs synthesized from endophytic fungi *Talaromyces purpureogenus* against bacterial pathogens

Pathogenic bacterial strains	Zone of inhibition (mm)				
	Vancomycin (5 µg/mL)	Silver nanoparticles (Tp-AgNPs)			
		25 µg/mL	50 µg/mL	75 µg/mL	100 µg/mL
S. aureus	9	6	7	8	9
B.cereus	22	8	9	10	11
S. enterica	20	8	9	9.5	11
P. aeruginosa	15	7.5	8	10.5	13
E. coli	8	8	8.5	9.5	11

Abbreviations: Tp-AgNPs, *Talaromyces purpureogenus* silver nanoparticles; *S. aureus, Staphylococcus* aureus; *B.cereus, Bcillus cereus; S.enterica, Salmonella entrica; P. aeruginosa, Pseudomonas aeruginosa;E.coli, Escherichia coli.*

analysis confirmed the presence of 38.15% of Ag atoms (Figure 2C–E).

Cell viability

The Tp-AgNPs showed cytotoxicity in A549 cells even at the lowest concentration of 2 μg/mL, and the cytotoxicity was also increased with the increase of NPs concentration (Figure 3A). Moreover, $AgNO_3$ showed higher cytotoxicity than the Tp-AgNPs. Further, the calculated IC_{50} for AgNPs and $AgNO_3$ was 376.24 and 250.31 μg/mL, respectively. According to the results of cell flow cytometer, 5.92% of cell apoptosis was induced by Tp-AgNPs (Figure 3B,C). Similarly, AgNPs are known to induce cytotoxicity on various cancer cells rat alveolar macrophages,[45] HepG2,[46] A549, SGC-7901, MCF7,[47] HeLa, U937, RAW 264.7, L929, A431, HIV virus.[48] Moreover, the cytotoxicity of the AgNPs depends on size, surface area, internalization and attachment efficiency. Smaller size of the AgNPs with smaller size can be able to internalize in the mammalian cells and cause the cytotoxicity through ROS generation, nucleus damage, activation of the apoptosis or mitochondrial pathways.[47] The potential cytotoxicity of Tp-AgNPs is attributed to smaller size of <50 nm in Tp-AgNPS, which not only reflected the cytotoxicity but also reflected in excellent anti-cancer activity.

Antibacterial

The Tp-AgNPs showed different degrees of antibacterial activity with increase in concentration (Figure 4). Our results on potent antibacterial activity of AgNPs are in accordance with earlier reports, as shown in Table 1. Tp-AgNPs significantly inhibited the growth of Gram-positive or Gram-negative pathogens at the minimal inhibitory concentration of 16.12 $\mu g.mL^{-1}$, and 13.98 $\mu g.mL^{-1}$, respectively. Moreover, Tp-AgNPs showed higher zone of inhibition against *S. aureus* (9 mm), *P. aeruginosa* (13 mm) and *E. coli* (11 mm) and it is similar to positive antibiotic control vancomycin (Table 2). TP-AgNPs did not show such a strong antibacterial effect on *B. cereus* (11 mm) and *S. enterica* (11 mm), which is similar to an antibiotic (Table 2).

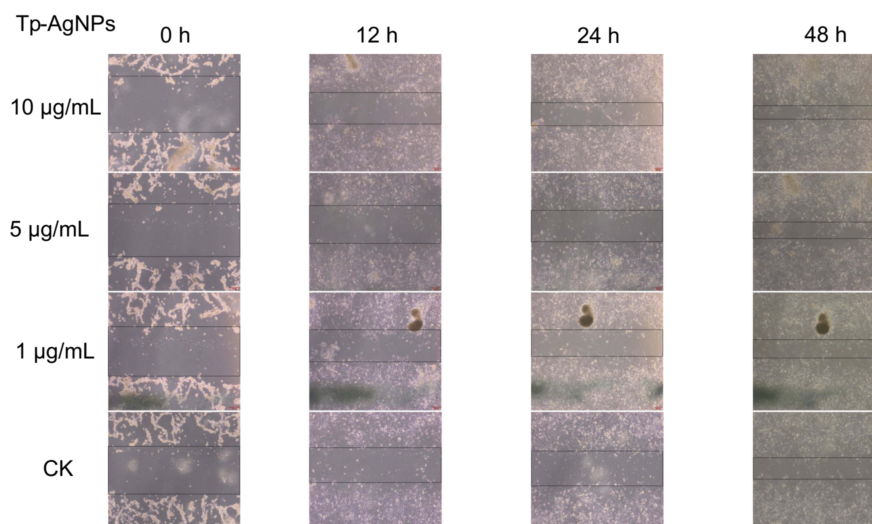

Figure 5 Wound healing effect of the Tp-AgNPs in NIH3T3 cells at different time intervals.
Abbreviations: CK, control group; Tp-AgNPs, *Talaromyces purpureogenus* silver nanoparticles; NIH3T3, Swiss albino mouse embryo tissue.

Table 3 Cell wound healing efficiency of Tp-AgNPs

Concentration of Tp-AgNPs (μg/mL)	Wound healing area (cm^2)			
	0 hrs	12 hrs	24 hrs	48 hrs
Untreated	5.244	3.8	3.79	2.356
1	5.434	3.487	2.888	1.976
5	5.776	4.18	3.42	1.824
10	6.156	3.42	2.546	1.436

Abbreviation: Tp-AgNPs, *Talaromyces purpureogenus* silver nanoparticles.

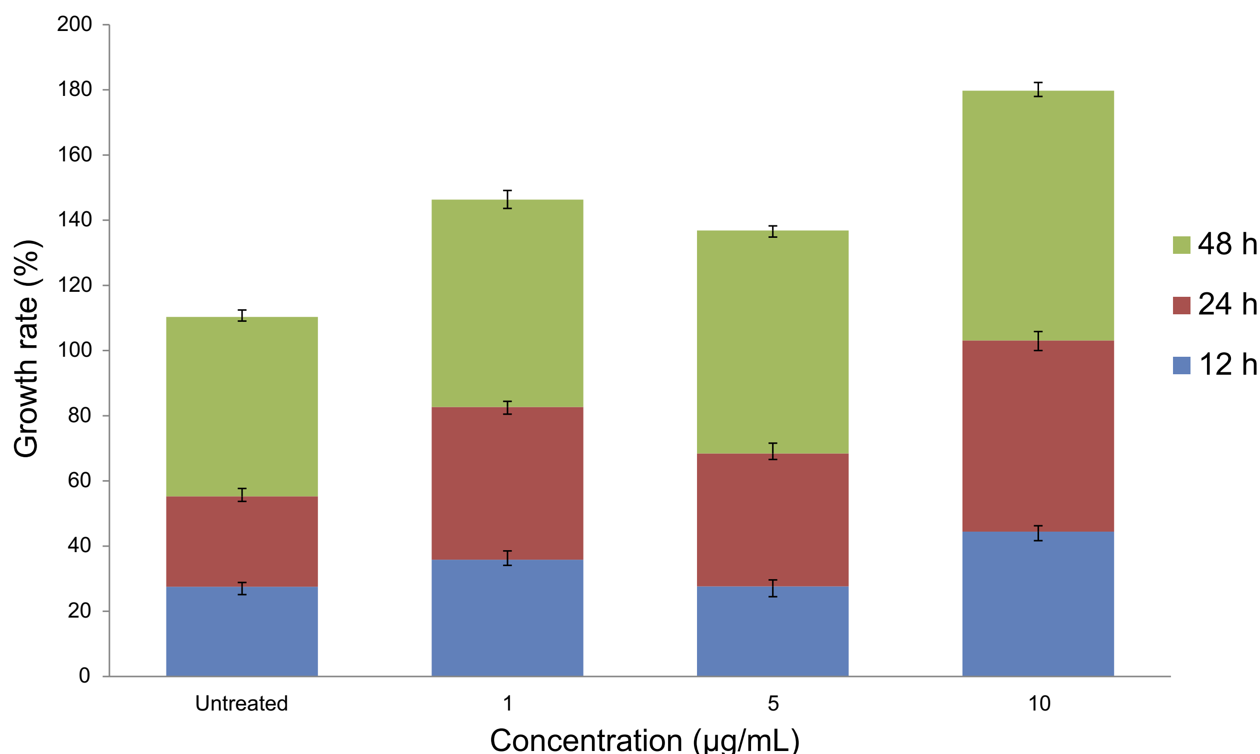

Figure 6 The growth rate of wound healing effort of the Tp-AgNPs in NIH3T3 cells at different time intervals.
Abbreviations: Tp-AgNPs, *Talaromyces purpureogenus* silver nanoparticles; NIH3T3, Swiss albino mouse embryo tissue.

Cell wound healing

Microscopic analysis revealed that the wound area decreased with the treatment of Tp-AgNPs as compared to the untreated control group after 48 hrs. The wound scratch distance of treated group was relatively small (Figure 5). The wound area decreased with the dose-dependent manner. For example, the wound area was 1.976, 1.824, and 1.4364 cm^2, respectively, at different concentrations (1, 5 and 10 μg/mL) of the experimental group. In addition, the wound area of treated group was smaller than the untreated control area (2.356 cm^2) (Table 3). By comparing the cell growth rate for each time period, the growth rate of each treated group was significantly higher than that of the untreated control (Figure 6). Tp-AgNPs were not toxic to NIH3T3 normal cells.

Conclusion

In this study, we synthesized Tp-AgNPs using MEEF and they were characterized for is high-quality crystal particles with a size <50 nm. The NPs showed the concentration-dependent cytotoxicity against A549 and have a good inhibitory effect on various pathogenic bacteria. In addition, the NPs also showed the cell wound healing efficiency. Further focus will be on the molecular mechanism of anti-cancer and antibacterial properties of Tp-AgNPs.

Acknowledgments

This work was supported by Korea Research Fellowship Program through the National Research Foundation of Korea (NRF) funded by the Ministry of Science, ICT and Future Planning (2017H1D3A1A01052610).

Disclosure

The authors declare no competing financial or other conflicts of interests in this work.

References

1. Thakkar KN, Mhatre SS, Parikh RY. Biological synthesis of metallic nanoparticles. *Nanomedicine*. 2017;6:257–262. doi:10.1016/j.nano.2009.07.002
2. Shanmuganathan R, MubarakAli D, Prabakar D, et al. An enhancement of antimicrobial efficacy of biogenic and ceftriaxone-conjugated silver nanoparticles: green approach. *Environ Sci Pollution Res*. 2018;25(11):10362–10370. doi:10.1007/s11356-017-9367-9
3. Pugazhendhi A, Prabakar D, Jacob JM, Karuppusamy I, Saratale RG. Synthesis and characterization of silver nanoparticles using Gelidium amansii and its antimicrobial property against various pathogenic bacteria. *Microb Pathog*. 2018;114:41–45. doi:10.1016/j.micpath.2017.11.013
4. Saravanan M, Barik SK, MubarakAli D, Prakash P, Pugazhendhi A. Synthesis of silver nanoparticles from Bacillus brevis (NCIM 2533) and their antibacterial activity against pathogenic bacteria. *Microb Pathog*. 2018;116:221–226. doi:10.1016/j.micpath.2018.01.038
5. Singh MR, Black K. Anomalous dipole–dipole interaction in an ensemble of quantum emitters and metallic nanoparticle hybrids. *J Phys Chem C*. 2018;122(46):26584–26591. doi:10.1021/acs.jpcc.8b06352
6. Singh MR, Chandra Sekhar M, Balakrishnan S, Masood S. Medical applications of hybrids made from quantum emitter and metallic nanoshell. *J Appl Phys*. 2017;122(3):034306. doi:10.1063/1.4994308
7. Singh MR, Guo J,J, Cid JM, De Hoyos Martinez JE. Control of fluorescence in quantum emitter and metallic nanoshell hybrids for medical applications. *J Appl Phys*. 2017;121(9):094303. doi:10.1063/1.4977756
8. Cox JD, Singh MR, von Bilderling C, Bragas AV. A nonlinear switching mechanism in quantum dot and metallic nanoparticle hybrid systems. *Adv Opt Mater*. 2013;1(6):460–467. doi:10.1002/adom.v1.6
9. Schindel D, Singh MR. A study of energy absorption rate in a quantum dot and metallic nanosphere hybrid system. *J Phy Condens Matter*. 2015;27(34):345301.
10. Singh D, Rathod V, Ninganagouda S, Herimath J, Kulkarni P. Biosynthesis of silver nanoparticles by endophytic fungi Pencillium sp. Isolated from Curcuma Longa (turmeric) and its antibacterial activity against pathogenic gram-negative bacteria. *J Pharm Res*. 2013;7:448–453. doi:10.1016/j.jopr.2013.06.003
11. Shah M, Fawcett D, Sharma S, Tripathy SK. G.E.J. Poinern Green synthesis of metallic nanoparticles via biological entities. *Materials*. 2015;8:7278–7308. doi:10.3390/ma8125486
12. Chernousova S, Epple M. Silver as antibacterial agent: ion, nanoparticle, and metal. *Angew Chem Int Ed Engl*. 2013;52:1636–1653. doi:10.1002/anie.201205923
13. Zhao XX, Zhou LF, Rajoka MSR, et al. Fungal silver nanoparticle: synthesis, application and challengess. *Crit Rev Biotechnol*. 2018;38(6):817–835. doi:10.1080/07388551.2017.1414141
14. Jena P, Mohanty S, Mallick R, Jacob B, Sonawane A. Toxicity and antibacterial assessment of chitosan-coated silver nanoparticles on human pathogens and macrophage cells. *Int J Nanomedicine*. 2012;7:1805-1818. doi: 10.2147/IJN.S28077..
15. Zhang L, Gu FX, Chan JM, Wang AZ, Langer RS, Farokhzad OC. Nanoparticles in medicine: therapeutic applications and developments. *Clin Pharmacol Ther*. 2008;83(5):761–769. doi:10.1038/sj.clpt.6100400
16. Le OB, Stellacci F. Antibacterial activity of silver nanoparticles: a surface science insight. *Nano Today*. 2015;10:339–354. doi:10.1016/j.nantod.2015.04.002
17. Bray F, Ferlay J, Soerjomataram I, Siegel RL, Torre LA, Jemal A. World cancer statistics. GLOBOCAN estimates of incidence and mortality worldwide for 36 cancers in 185 countries. *CA Cancer J Clin* 2018;68(6):394–424. doi:10.3322/caac.21492
18. Giard DJ, Aaronson SA, Todaro GJ, et al. In vitro cultivation of human tumors: establishment of cell lines derived from a series of solid tumors. *J Natl Cancer Inst*. 1973;51(5):1417–1423. doi:10.1093/jnci/51.5.1417
19. Pugazhendhi A, Edison TNJI, Karuppusamy I, Kathirvel B. Inorganic nanoparticles: a potential cancer therapy for human welfare. *Int J Pharm*. 2018;539(1):104–111. doi:10.1016/j.ijpharm.2018.01.034
20. Coccia M, Wang L. Path-breaking directions of nanotechnology-based chemotherapy and molecular cancer therapy. *Technol Forecast Soc Change*. 2015;94:155–169. doi:10.1016/j.techfore.2014.09.007
21. Estanqueiro M, Amaral MH, Conceicao J, Sousa LJM. Nanotechnological carriers for cancer chemotherapy, The state of the art. *Colloids Surf B*. 2015;126:631–648. doi:10.1016/j.colsurfb.2014.12.041
22. Santoni M, Massari F, Del Re M, et al. Investigational therapies targeting signal transducer and activator of transcription 3 for the treatment of cancer. *Expert Opin Invest Drugs*. 2015;24:809–824. doi:10.1517/13543784.2015.1020370
23. Wang C, Makila EM, Kaasalainen MH, et al. Dual-drug delivery by porous silicon nanoparticles for improved cellular uptake., sustained release., and combination therapy. *Acta Biomater*. 2015;16:206–214. doi:10.1016/j.actbio.2015.01.021
24. Devanesan S, AlSalhi MS, Vishnubalaji R. Rapid biological synthesis of silver nanoparticles using plant seed extracts and their cytotoxicity on colorectal cancer cell lines. *J Clust Sci*. 2017;28:595–605. doi:10.1007/s10876-016-1134-4
25. Nakkala JR, Mata R, Sadras SR. Green synthesized nano silver: synthesis, physicochemical profiling, antibacterial, anticancer activities and biological in vivo toxicity. *J Colloid Interface Sci*. 2017;499:33–45. doi:10.1016/j.jcis.2017.03.090
26. Preetha D, Prachi K, Chirom A. Synthesis and characterization of silver nanoparticles using cannonball leaves and their cytotoxic activity against MCF-7 cell line. *J Nanotechnol*. 2013;2:421–428.
27. Kulkarni RR, Shaiwale NS, Deobagkar DN. Synthesis and extracellular accumulation of silver nanoparticles by employing radiation-resistant Deinococcus radiodurans, their characterization, and determination of bioactivity. *Int J Nanomed*. 2015;10:963–974.
28. Mishra Y, Singh A, Batra A, Sharma MM. Understanding the biodiversity and biological applications of endophytic fungi: a review. *J Microb Biochem Technol*. 2014;S8:004.
29. Ma L, Su W, Liu JX, et al. Optimization for extracellular biosynthesis of silver nanoparticles by *Penicillium aculeatum Su1* and their antimicrobial activity and cytotoxic effect compared with silver ions. *Mater Sci Eng C*. 2017;77:963–971. doi:10.1016/j.msec.2017.03.294
30. Saravanakumar, K., Shanmugam S., Varukattu N.B, et al. Biosynthesis and characterization of copper oxide nanoparticles from indigenous fungi and its effect of photothermolysis on human lung carcinoma. *J Photochem Photobiol B*. 2019;190:103–109. doi:10.1016/j.jphotobiol.2018.02.005
31. Saravanakumar K, Wang M-H. Trichoderma based synthesis of anti-pathogenic silver nanoparticles and their characterization, antioxidant and cytotoxicity properties. *Microb Pathog*. 2018;114:269–273. doi:10.1016/j.micpath.2017.12.005

32. Shukla H, Sandhu SS. Mycofabrication and characterization of silver nanoparticles by using some endophytic fungi with special reference to their antimicrobial potential. *Int J Nanotechnol Appl*. 2017;7:7–22.
33. Johnson PB, Christy RW. Optical constants of the noble metals. *Phys Rev B*. 1972;6(12):4370–4379. doi:10.1103/PhysRevB.6.4370
34. Xu J, Han X, Liu H, Hu Y. Synthesis and optical properties of silver nanoparticles stabilized by gemini surfactant. *Colloids Surf A*. 2006;273(1–3):179–183. doi:10.1016/j.colsurfa.2005.08.019
35. Saravanakumar, K., Jeevithan E, Chelliah R, et al. Zinc-chitosan nanoparticles induced apoptosis in human acute T-lymphocyte leukemia through activation of tumor necrosis factor receptor CD95 and apoptosis-related genes. *Int J Biol Macromol*. 2018;119:1144–1153. doi:10.1016/j.ijbiomac.2018.08.017
36. Brumfitt W, Hamilton-Miller JM, Franklin I. Antibiotic activity of natural products: 1. *Propolis Microbios*. 1990;62(250):19–22.
37. Ahmad N, Sharma S, Alam MK, et al. Rapid synthesis of silver nanoparticles using dried medicinal plant of basil. *Colloids Surf B*. 2010;81(1):81–86. doi:10.1016/j.colsurfb.2010.06.029
38. Singh MR, Schindel DG, Hatef A. Dipole-dipole interaction in a quantum dot and metallic nanorod hybrid system. *Appl Phys Lett*. 2011;99(18):181106. doi:10.1063/1.3658395
39. Hatef A, Sadeghi SM, Singh MR. Coherent molecular resonances in quantum dot–metallic nanoparticle systems: coherent self-renormalization and structural effects. *Nanotechnology*. 2012;23(20):205203. doi:10.1088/0957-4484/23/20/205203
40. Saravanakumar, K., Chelliah R, Shanmugam S, et al. Green synthesis and characterization of biologically active nanosilver from seed extract of Gardenia jasminoides Ellis. *J Photochem Photobiol B*. 2018;185:126–135. doi:10.1016/j.jphotobiol.2018.05.032
41. Deene M, Lingappa K. Microwave assisted rapid and green synthesis of silver nanoparticles using a pigment produced by *Streptomyces coelicolor* klmp33. *Bioinorg Chem Appl*. 2013;2013: Article 341798.
42. Pavani KV, Gayathramma K, Aparajitha B, Shah S. Phyto-synthesis of silver nanoparticles using extracts of ipomoea indica flowers. *Am J Nanomater*. 2013;1(1):2013.
43. Aravinthan A, Govarthanan M, Selvam K, et al. Sunroot mediated synthesis and characterization of silver nanoparticles and evaluation of its antibacterial and rat splenocyte cytotoxic effects. *Int J Nanomed*. 2015;10:1977–1983. doi:10.2147/IJN.S79106
44. Fadel QJ, Al-Mashhedy LAM. Biosynthesis of silver nanoparticles using peel extract of Raphanus sativus L. *Biotechnol Ind J*. 2017;13(1):120.
45. Carlson, C, Hussain SM, Schrand AMK, et al. Unique cellular interaction of silver nanoparticles: size-dependent generation of reactive oxygen species. *J Phy Chem B*. 2008;112(43):13608–13619. doi:10.1021/jp712087m
46. Mishra, AR, Zheng J, Tang X, et al. Silver nanoparticle-induced autophagic-lysosomal disruption and NLRP3-Inflammasome Activation in HepG2 cells is size-dependent. *Toxicol Sci*. 2016;150(2):473–487. doi:10.1093/toxsci/kfw011
47. Liu, W, Wu Y, Wang C, et al. Impact of silver nanoparticles on human cells: effect of particle size. *Nanotoxicology*. 2010;4(3):319–330. doi:10.3109/17435390.2010.483745
48. Akter, M, Sikder MT, Rahman MM, et al. A systematic review on silver nanoparticles-induced cytotoxicity: physicochemical properties and perspectives. *J Adv Res*. 2018;9:1–16. doi:10.1016/j.jare.2017.10.008
49. Ottoni CA, Simoes MF, Fernandes S, et al. Screening of filamentous fungi for antimicrobial silver nanoparticles synthesis. *AMB Expr*. 2017;7(31). doi:10.1186/s13568-017-0332-2
50. Tahira A, Mohd SK, Hemalatha S. A facile and rapid method for green synthesis of Silver Myco nanoparticles using endophytic fungi. *Int J Nano Dimension*. 2018;9(4):435–441.
51. Mohamed MA, HUSSEIN HM ALIAAM. Antifungal activity of different size controlled stable silver nanoparticles biosynthesized by the endophytic fungus Aspergillus terreus. *J Phytopathology Pest Manag*. 2018;5(2):88–107.
52. Prabu KS, Rajkuberan C, Sathishkumar G, et al. Antimicrobial and larvicidal activity of eco-friendly silver nanoparticles synthesized from endophytic fungi *Phomopsis liquidambaris*. *Biocata Agricl Biotechnol*. 2018;16:22–30. doi:10.1016/j.bcab.2018.07.006
53. Mohammad F, Saeed F. Biosynthesis of antibacterial silver nanoparticles by endophytic fungus *Nemania* sp. Isolated From Taxus baccata L.(Iranian Yew). *Zahedan J Res Med Sci*. 2018;20(6):e57916.
54. Sahadevan N, Sebastian JM, Sunil MA, Soman S, Radhakrishnan EK, Mathew J. Efficient visible light induced synthesis of silver nanoparticles by *Penicillium polonicum* ARA 10 isolated from *Chetomorpha antennina* and its antibacterial efficacy against *Salmonella* enterica serova *Typhimurium*. *J Photochem Photobiol B*. 2018;180:175–185. doi:10.1016/j.jphotobiol.2018.02.005
55. Balakumaran MD, Ramachandran R, Kalaichelvan PT. Exploitation of endophytic fungus, *Guignardia mangiferae* for extracellular synthesis of silver nanoparticles and their *in vitro* biological activities. *Microbiol Res*. 2015;178:9–17. doi:10.1016/j.micres.2015.05.009
56. Hemashekhar B, Chandrappa CP, Govindappa M, Chandrasekhar N, Nagaraju G, Ramachandra YL. Green synthesis of silver nanoparticles from Endophytic fungus *Aspergillus niger* isolated from *Simarouba glauca* leaf and its Antibacterial and Antioxidant activity. *Inter J Eng Res Appl*. 2017;7(8):17–24.
57. Reena R, Dushyant S, Monika C, Yadav JP. Green synthesis, characterization and antibacterial activity of silver nanoparticles of endophytic fungi *Aspergillus terreus*. *J Nanomed Nanotechnol*. 2017;8:4.
58. Shaheen TI, Abeer AAEA. In-situ green myco-synthesis of silver nanoparticles onto cotton fabrics for broad spectrum antimicrobial activity. *Int J Biol Macromol*. 2018;118:2121–2130. doi:10.1016/j.ijbiomac.2018.07.062
59. Singh DK, Kumar J, Sharma VK, et al. Mycosynthesis of bactericidal silver and polymorphic gold nanoparticles–physicochemical variation effects and mechanism. *Nanomadicine*. 2018;13(2):191–207.
60. Vivian C, Lisa OGA, Tong KS. Synthesis of silver nanoparticles mediated by endophytic fungi associated with orchids and its antibacterial activity. *Materials Today: Proceedings*. 2018;5(10;Part 2):22093–22100.
61. Tej S, Kumari J, Amar P, Ajeet S, Ranchan C, Chandel SS. Biosynthesis, characterization and antibacterial activity of silver nanoparticles using an endophytic fungal supernatant of Raphanus sativus. *J Genetic Eng Biotechnol*. 2017;15:31–39. doi:10.1016/j.jgeb.2017.04.005
62. Govindappa M, Farheen H, Chandrappa CP, Channabasava RVR, Vinay BR. Mycosynthesis of silver nanoparticles using extract of endophytic fungi, Penicillium species of Glycosmis mauritiana, and its antioxidant, antimicrobial, anti-inflammatory and tyrokinase inhibitory activity. *Adv Nat Sci*. 2016;7(3):Article035014.
63. Vardhana J, Kathiravan G. Biosynthesis of silver nanoparticles by endophytic fungi Pestaloptiopsis pauciseta isolated from the leaves of *Psidium guajava* linn. *Int J Pharm Sci Rev Res*. 2015;31(1):29–31.
64. Parthasarathy R, Sathiyabama M, Prabha T. Biosynthesis of silver nanoparticles using an endophytic fungus, Curvularia lunata and its antimicrobial potential. *J Nanosci Nanoeng*. 2015;1(4):241–247.
65. Vasudeva RN, Pushpalatha B, Sukhendu BG, Vijaya T. Endophytic fungal assisted synthesis of silver nanoparticles, characterization, and antimicrobial activity. *Asian J Pharm Clinl Res*. 2015;8(3):113–116.
66. Lamabam SD, Joshi SR. Ultrastructures of silver nanoparticles biosynthesized using endophytic fungi. *J Microsc Ultrastruct*. 2015;3:29–37. doi:10.1016/j.jmau.2014.10.004

67. Dattu S, Vandana R, Shivaraj N, Jyothi H, Ashish KS, Jasmine M. Optimization and characterization of silver nanoparticle by endophytic fungi *Penicillium* sp. Isolated from *Curcuma longa* (Turmeric) and application studies against MDR *E. coli* and *S. aureus*. *Bioinorg Chem Appl*. 2014;2014:Article 40S021.
68. Rodrigues AG, Ping LY, Marcato PD, et al. Biogenic antimicrobial silver nanoparticles produced by fungi. *Appl Microbiol Biotechnol*. 2013;97:775–782. doi:10.1007/s00253-012-4209-7

International Journal of Nanomedicine Dovepress

Publish your work in this journal

The International Journal of Nanomedicine is an international, peer-reviewed journal focusing on the application of nanotechnology in diagnostics, therapeutics, and drug delivery systems throughout the biomedical field. This journal is indexed on PubMed Central, MedLine, CAS, SciSearch®, Current Contents®/Clinical Medicine, Journal Citation Reports/Science Edition, EMBase, Scopus and the Elsevier Bibliographic databases. The manuscript management system is completely online and includes a very quick and fair peer-review system, which is all easy to use. Visit http://www.dovepress.com/testimonials.php to read real quotes from published authors.

Submit your manuscript here: https://www.dovepress.com/international-journal-of-nanomedicine-journal